Eur. Phys. J. B **9**, 335–341 (1999)

THE EUROPEAN PHYSICAL JOURNAL B

EDP Sciences

Surface waves in ferrofluids under vertical magnetic field

J. Browaeys[1,2,a], J.-C. Bacri[1,2], C. Flament[1,2], S. Neveu[3], and R. Perzynski[1,2]

[1] Équipe Ferrofluide de l'Université Paris 7 (case 70.08), 2 place Jussieu, 75251 Paris Cedex 05, France
[2] Laboratoire des Milieux Désordonnés et Hétérogènes[b], Université Pierre et Marie Curie (Paris VI), case 78, 4 place Jussieu, 75252 Paris Cedex 05, France
[3] Laboratoire des Liquides Ioniques et Interfaces Chargées[c], Université Pierre et Marie Curie (Paris VI), Bâtiment F, case 63, 4 place Jussieu, 75252 Paris Cedex 05, France

Received 11 May 1998

Abstract. We present here new experimental results about the waves at the horizontal free surface of a magnetic fluid submitted to a normal magnetic field. The waves are generated by a small modulation at frequency ω of the vertical field H^e. Using a shadowgraph method, we are able to measure the wavevector k of the 2D waves for a given value of ω and H^e. The dispersion relation of the surface waves is established experimentally. On the other hand, we propose a theoretical derivation of the dispersion equation which includes a more complete treatment of the magnetic term than the previous works. Finally, we conclude that a linear and inviscid analysis is sufficient to fit well the experimental data, except in the vicinity of the critical field where a surface instability occurs.

PACS. 75.50.Mm Magnetic liquids – 47.35.+i Hydrodynamic waves – 68.10.-m Fluid surfaces and fluid-fluid interface

1 Introduction

A ferrofluid is a stable colloidal suspension of magnetic particles. It behaves as a normal fluid except that it can experience forces due to magnetic polarization: its magnetic susceptibility is giant, usually in the order of unity.

The dispersion equation of capillary/gravity waves at the free surface of a ferrofluid in the presence of a normal magnetic field presents many interesting features. It is already well known that above a certain critical field the surface spontaneously deforms into regularly spaced peaks [1]: the so-called normal field or Rosensweig instability is usually modeled using the linear analysis which leads to the dispersion equation. At the critical field H_c, the dispersion curve adjoins the zero frequency axis at a non zero wavelength (usually close to the capillary wavelength). The linear analysis is unable to explain the pattern which is hexagonal just above the threshold and sometimes square [2] for higher magnetic fields: this phenomenon has already been the subject of numerous theoretical [3], numerical [4] and experimental [5] studies. In this study we focus our interest on the behavior of the surface waves below this critical field.

The dispersion curve actually exhibits a peculiar feature. It is possible to define another critical field (H^*, lower than H_c) above which the dispersion curve is no more monotonic. Above this field, waves are still stable but the dispersion curve $\omega(k)$ presents a minimum so that the group velocity can be negative; in principle three wave numbers could be selected for a given frequency. It is interesting to note the analogy between the minimum on this dispersion curve and the roton minimum in the energy spectrum of superfluid helium [6].

The precise knowledge of the dispersion equation is also of paramount importance for any process that is sensitive to surface instabilities, such as the jet instability [7]. In the first published experimental study [8] surface waves were induced by a spatial forcing: standing waves were established by regularly shaking a ferrofluid container. The experiment was realized in the presence of an inadvertent gradient of magnetic field, which implied the use of a modified dispersion equation. Moreover the number of experimental data was not large enough to precisely assess the theory. Recently waves induced by a temporal forcing were studied in a one-dimensional ring geometry [9], but due to this particular configuration no quantitative check of the theory has been able to be performed. To our knowledge this study is the first quantitative and extensive test of the theoretical dispersion equation.

2 Dispersion equation

Cowley and Rosensweig [1,10] were the first to study the peak instability at the free surface of a magnetic fluid. Although they didn't actually express the dispersion

[a] e-mail: `browaeys@ccr.jussieu.fr`
[b] UMR 7603 (CNRS)
[c] UMR 7612 (CNRS)

equation for waves at the free surface of a ferrofluid (they were interested in the threshold value of the magnetic field at which the peaks form), they developed the linear theory which allows to directly derive the magnetic term in the dispersion equation. They considered that the ferrofluid was inviscid, that its depth was infinite and that it was infinitely extended in the horizontal direction [11]. Zelazo and Melcher [8] refined this analysis: they considered waves at the interface of two non-miscible magnetic fluid layers of arbitrary depth and explicitly wrote the dispersion equation. However, the boundary condition they used, *i.e.* placing infinitely magnetically permeable materials above and underneath the fluid is not of practical use (at least for the visualization of the interface). More recently, Abou *et al.* [12] changed this boundary condition (the layer is actually surrounded by free space), and included the effect of viscosity. However, they omitted to take into account the demagnetization coefficient and also supposed that the permeability of the material was constant, a fact that is not supported experimentally, since a magnetization saturation exists in the material.

Following step by step the method of Zelazo and Melcher [8], but considering free space as the boundary condition of the ferrofluid layer, we derive the dispersion equation for an inviscid layer of ferrofluid of any thickness. Let M be the magnetization of the ferrofluid layer, h its thickness, ρ its density, σ its surface tension, μ_0 the vacuum permeability and g the gravitational acceleration. Two magnetic composite quantities related to the magnetization curve of the ferrofluid $M(H^{\mathrm{i}})$ (H^{i} is the magnetic field inside the ferrofluid) appear in the calculation:

$$r = \sqrt{\left(1 + \frac{M(H^{\mathrm{i}})}{H^{\mathrm{i}}}\right)\left(1 + \frac{\mathrm{d}M}{\mathrm{d}H}(H^{\mathrm{i}})\right)} \tag{1}$$

$$s = \sqrt{\frac{1 + \frac{M(H^{\mathrm{i}})}{H^{\mathrm{i}}}}{1 + \frac{\mathrm{d}M}{\mathrm{d}H}(H^{\mathrm{i}})}}. \tag{2}$$

The magnetic field H^{i} is computed from the externally applied magnetic field H^{e} by the resolution of an implicit equation [13] :

$$H^{\mathrm{e}} = M(H^{\mathrm{i}}) + H^{\mathrm{i}}. \tag{3}$$

The analysis with normal modes of perturbation leads to an equation linking the pulsation ω to the modulus k of the wavevector:

$$\omega^2 = \frac{\tanh(kh)}{\rho}\left(\rho g k + \sigma k^3 - \mu_0 M^2 k^2 \frac{r}{r+1}\left(\frac{1 - \left(\frac{r-1}{r+1}\right)\exp(-2skh)}{1 - \left(\frac{r-1}{r+1}\right)^2 \exp(-2skh)}\right)\right). \tag{4}$$

This result is compatible with Abou's [12] for an inviscid fluid, provided the permeability of the fluid is set constant and the demagnetization taken into account in (4) [14]. In the equation that Abou *et al.* propose, magnetic and viscous effects are not directly coupled, so it is possible to derive a more complete dispersion equation integrating viscous effects: a simple substitution of our magnetic term (right side of Eq. (4)) to theirs leads to the result. Due to the complexity, and because viscosity effects may be neglected as we show further on, we do not present this equation here.

To quantify the effect of viscosity, it is possible to define two Reynolds numbers [12], either based on the depth of the ferrofluid layer, or based on the wavelength:

$$Re = \frac{\omega h^2}{\nu} \tag{5}$$

or

$$Re = \frac{\omega}{\nu k^2}\cdot \tag{6}$$

The influence of viscosity on the flow generated by surface waves is negligible provided the Reynolds number is greater than 10 [15]. This leads to two conditions for the pulsation ω for short and long wavelengths. In the following we show that these two conditions are verified in our experiment:

$$\omega > \sup\left(10\frac{\nu}{h^2}, 10\nu k^2\right)\cdot \tag{7}$$

The influence of the thickness of the layer on the dispersion equation depends on the value of the wavelength. If the wavelength is small compared to the thickness, that is $kh \gg 1$, we are in the asymptotic regime of infinite thickness. In this limit and considering that the permeability of the magnetic fluid is constant, equation (4) simplifies:

$$\omega^2 = gk + \frac{\sigma k^3}{\rho} - \frac{\mu_0 {H^{\mathrm{e}}}^2 k^2}{\rho}\left(\frac{\chi^2}{(1+\chi)(2+\chi)}\right)\cdot \tag{8}$$

It is then possible to analytically derive H_{c} and H^*:

$$\omega = 0 \text{ and } \frac{\partial\omega}{\partial k} = 0 \Rightarrow H_{\mathrm{c}} = \sqrt{\frac{2(1+\chi)(2+\chi)}{\chi^2}\frac{\sqrt{\rho g\sigma}}{\mu_0}} \tag{9}$$

$$\frac{\partial\omega}{\partial k} = 0 \text{ and } \frac{\partial^2\omega}{\partial k^2} = 0 \Rightarrow H^* = \sqrt[4]{\frac{3}{4}} H_{\mathrm{c}} \approx 0.93\ H_{\mathrm{c}}. \tag{10}$$

With this approximation, the critical wavelength k_{c} at the threshold of the peak instability is equal to the capillary wavelength; we define a characteristic pulsation ω_{c} as the pulsation corresponding to the capillary wavelength without any magnetic field

$$k_{\mathrm{c}} = \sqrt{\frac{\rho g}{\sigma}} \tag{11}$$

and

$$\omega_{\mathrm{c}} = 2\left(\frac{\rho g^3}{\sigma}\right)^{1/4}\cdot \tag{12}$$

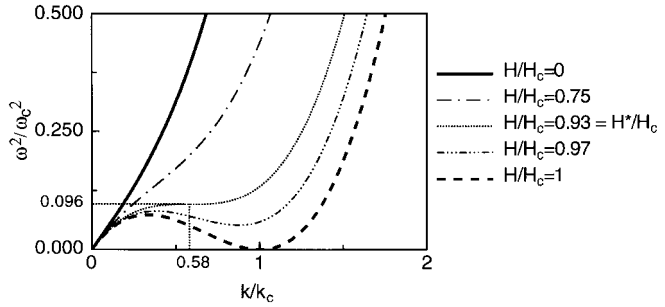

Fig. 1. Theoretical dispersion equation in the limit of infinite thickness for an inviscid ferrofluid. H_c represents the critical field of the peak instability; ω_c is the pulsation at the capillary wavelength for a null field. The curves are not monotonic anymore provided $H > 0.93H_c = H^*$.

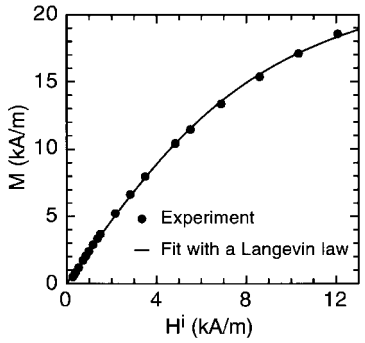

Fig. 2. Magnetization curve of the ferrofluid sample. The best least square fit with equation (16) gives $A_0 = 26.15$ kA/m and $A_1 = 3.63$ kA/m.

It is then possible to rewrite the dispersion equation in a non-dimensional form :

$$\left(\frac{\omega}{\omega_c}\right)^2 = \frac{1}{2}\left(\frac{k}{k_c} + \left(\frac{k}{k_c}\right)^3\right) - \left(\frac{H}{H_c}\right)^2 \left(\frac{k}{k_c}\right)^2. \quad (13)$$

Let k^* and ω^* respectively correspond to the wave vector modulus and pulsation at the bifurcation towards a non-monotonic dispersion curve; we have:

$$\frac{k^*}{k_c} = \frac{\sqrt{3}}{3} \approx 0.58 \quad (14)$$

and

$$\frac{\omega^{*2}}{\omega_c^2} = \frac{\sqrt{3}}{18} \approx 0.096. \quad (15)$$

We have drawn in Figure 1 the normalized dispersion curves for different magnetic field ratios H/H_c.

3 Experimental setup

3.1 Characteristics of the ferrofluid sample

We use an ionic ferrofluid synthesized according to Massart's method [16,17]. It is composed of a colloidal suspension of cobalt ferrite particles in water. Its density is

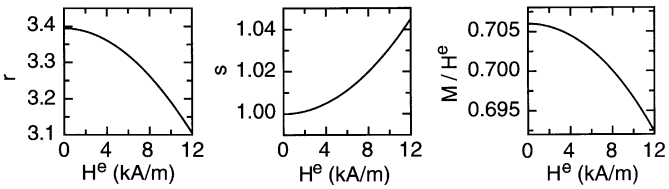

Fig. 3. Variation of magnetic characteristics of the sample with the external magnetic field.

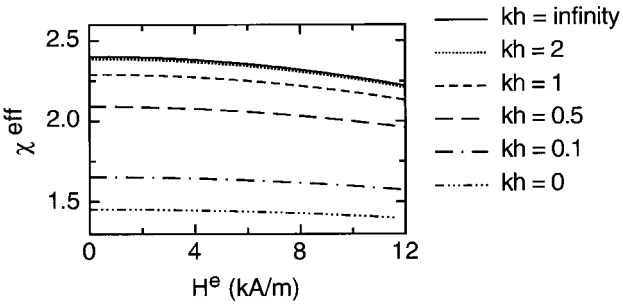

Fig. 4. Effective magnetic susceptibility χ_{eff} in function of the external magnetic field H^e for different non-dimensional wavevectors kh.

$\rho = 1560$ kg/m^3 and the deduced volume fraction of particles is 14%. Its surface tension with air, carefully measured with a Krüss K10T ring tensiometer, is 71.4 mN/m at 20 °C. This value is very close to the surface tension of water (73.2 mN/m), in agreement with the fact that our ionic ferrofluid is free of surfactant. The magnetization curve has been obtained by the use of a calibrated fluxmeter (Fig. 2). Because our ferrofluid is highly concentrated and polydisperse, it is unlikely to follow a classical Langevin paramagnetic curve. However, this approximation may stand for the range of magnetic field amplitude of our interest (from 0 to about 12 kA/m, the field around which the peaks instability develops):

$$M \approx A_0(\coth(H^i/A_1) - A_1/H^i). \quad (16)$$

It should be noted that the A_0 value obtained is *a priori* different from the magnetization saturation of the ferrofluid sample. The knowledge of the parameters of the fit A_0 and A_1 allows us to compute all the magnetic parameters of the problem, that is r, s and M in function of H^e. In Figure 3 it can be seen that the influence of the externally applied magnetic field on these three quantities is very small.

Let us introduce an effective susceptibility χ^{eff} as a function of the external magnetic field and of the non-dimensional product kh. This χ^{eff} value is computed so that the magnetic terms in equations (4, 8) give the same value. It is a measurement of the discrepancy when the magnetic term of (8) is misused. The following plot (Fig. 4) shows that the value of χ^{eff} is almost independent of the magnetic field thus justifying *a posteriori* the use of a simplified magnetic term (*i.e.* χ constant); on the other hand it shows that the dependence of the magnetic term on the thickness of the layer has to be accounted for. The dynamic viscosity of the sample, measured with

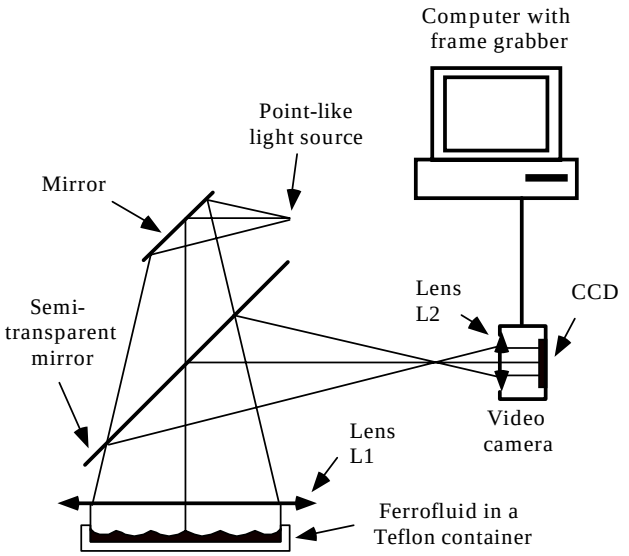

Fig. 5. Shadowgraph method. The amplitude of the wave has been exaggerated for the purpose of the sketch.

a Poiseuille viscometer, is 20 mPa s which leads to a kinematic viscosity of $\nu = 1.28 \times\ 10^{-5}$ m^2/s. In our experiment, viscosity effects may be neglected (see Sect. 4).

3.2 Experiment design

A circular Teflon® dish of 20 cm in diameter that contains the ferrofluid is placed between two horizontal coils (inner diameter is 25 cm, outer diameter 50 cm and thickness 11 cm); they produce the static vertical magnetic field and are arranged such as to ensure a 99% horizontal spatial homogeneity of the field (the gap between the coils is 6.5 cm wide). It should be pointed that the maximum observable wavelength is of same order as the radius of the vessel.

For our experiment, we need a very sensitive optical method to detect the wave amplitude. The shadowgraph method [18] is satisfactory since this afocal system is sensitive enough to detect 60 μm amplitude ripples. The ferrofluid surface is illuminated by a parallel light beam coming from a point-like source (an optical fiber illuminator) at the focal distance of lens L1. The camera lens L2 is placed in order to provide a parallel light beam to the CCD detector (see Fig. 5). The distance d between the CCD and the camera lens is set such as to focus just beneath or above the ferrofluid surface. The curved parts of the surface act as virtual lenses, and appear lightened or darkened on the video screen whether the curvature is positive or negative.

The first technique used for the production of surface waves consists in taking advantage of the magnetic properties of the fluid and use a local perturbation of the magnetic field as a mechanical perturbation; this is realized by placing a small coil beneath the ferrofluid container. One of the main drawbacks is that it is very difficult to excite waves the wavelength of which is small compared to the excitation coil size (about 2 cm in diameter). The same problem would manifest if the excitation was realized by oscillating a small permanent magnet near the surface.

Another way to achieve the excitation is to tap the ferrofluid surface with a small tip connected to a mechanical vibrator. Alternatively a small loudspeaker could have been used for the same purpose [9]. Although this is more adapted to the high frequency domain, it fails to produce long wavelength (typically longer than 2 cm).

The application of a small sinusoidal modulation in the vertical field creates propagative circular waves emitted by the edges due to magnetic forces in the meniscus. Figure 6 represents the spatio-temporal diagram of such waves. Because of the viscous damping [19], no stationary waves are observed, except in the center of the ferrofluid container. This effect may be a source of errors in Faraday instability waves experiments [20].

This method is very reliable for the production of waves in the interesting frequency range (3–25 Hz). The undulating component is merely 0.5% of the threshold field H_c. It is then difficult to extrapolate the results at fields lower than $0.1H_c$ where the undulation ratio is already 5%. These three methods give similar results. We exclusively used the third technique for the experiments because it is the only one adapted to the low frequency range (< 7 Hz).

4 Results

In order to represent experimental results and to fit parameters of the theoretical wave dispersion equation, we chose two cuts in the $(k, \omega, \mu_0 H^2)$ space of parameters (Figs. 7 and 8). The only parameter allowed to vary is the surface tension, because of its sensitivity to contaminants. All other parameters (the magnetic quantities, the density and the thickness of the ferrofluid layer) are set to their previously measured values. We have drawn in Figure 7 the frequency/wavelength domain where the effects of viscosity could be neglected. Our experimental points lie outside of this zone.

The fit for any value of ω and H leads to an average surface tension of 60 mN/m, which is 16% lower than the carefully measured value obtained from a ring tensiometer. The natural contamination of the surface by atmospheric dust behaving as a surfactant may explain this discrepancy. We thus perform another tensiometer measurement by letting the ferrofluid surface rest in an unpurified atmosphere: after a few minutes, the measured surface tension is only 52 mN/m. This static value is sensibly smaller than the result obtained in our experiment: it is known that dynamic measurements often lead to higher values [21]. For this reason, and since the surface tension is extremely sensitive on the presence of any surfactant (the quantity of which is not determined), the fitted value has to be understood as an *in situ* value, compatible with tensiometer measurements.

In a first experiment the magnetic field is set to different values and the wavevector measured as a function of frequency. The experimental dispersion is presented in Figure 7. The fits are satisfactory, although it is difficult

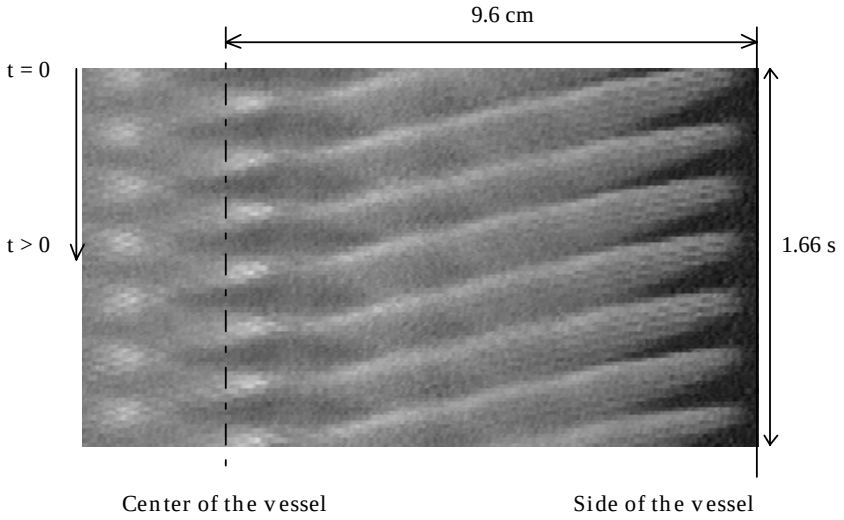

Fig. 6. Spatio temporal diagram of 4 Hz progressive surface waves at $H = 0.48H_c$. Each horizontal line of this diagram represents the profile of the surface in grey levels along a diameter cut of the ferrofluid vessel at a given time. White represents crests and black troughs. Waves are stationary close to the center.

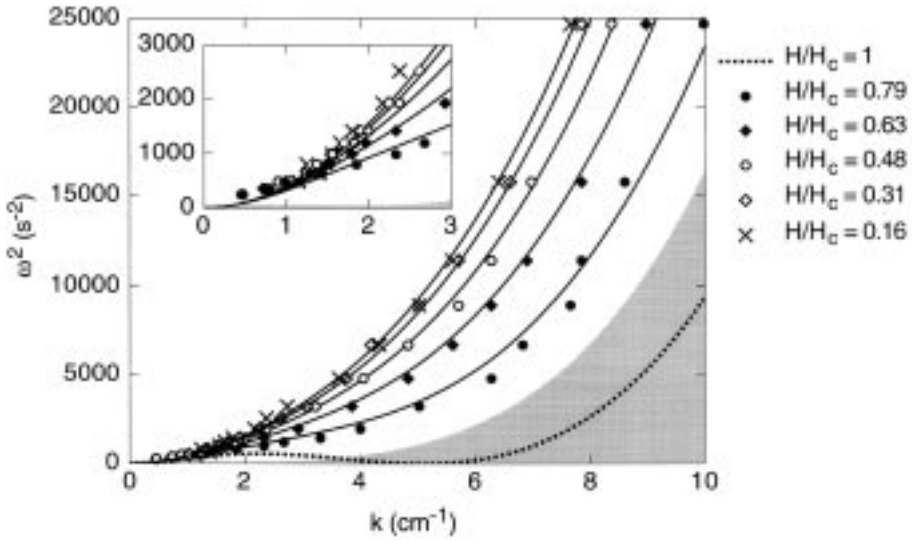

Fig. 7. Experimental dispersion equation in the (k, ω^2) plane for different magnetic fields. The black lines represent the theoretical dispersion equations with $\sigma = 60$ mN/m. The dotted line is the theoretical dispersion equation at the threshold field. The shaded area represents the frequency domain where viscosity effects become non negligible (Re <10).

to make any assertion when the wavevector is smaller than 3 cm^{-1}. The critical field is estimated from the fits: as we will see later on, it is extremely difficult to define a precise value of the threshold magnetic field H_c in our particular system. The maximum experimented value of the ratio H/H_c is voluntarily limited to 0.79 because above this field, peaks form at the boundary of the ferrofluid vessel; during the time of the experiment, the fluid in the peaks would dry and become lumpy. This is why it is better to set the frequency to different fixed values, and measure the wavelength as a function of the magnetic field. The corresponding results are presented in Figure 8. This plot is more discriminating, especially in the low wavelength domain ($k < 3$ cm^{-1}). Here it can be seen that the fit is not compatible with the experimental data especially in the region where the dispersion curve is non monotonic.

In this region, where the magnetic field is close to H_c, an unexpected static circular pattern develops (Figs. 9 and 10). It actually becomes visible (amplitude of the deformation exceeds 60 μm) as soon as the magnetic field exceeds half of the threshold value. Only the precision of the shadowgraph method allows to see such a deformation of the surface. The pattern is independent of the magnetic field, only the amplitude of the deformation increases with the magnetic field intensity. A possible explanation would be that the effective magnetic field is inhomogeneous because of the finite horizontal size of the sample (the demagnetization factor is not rigorously equal to one and depends

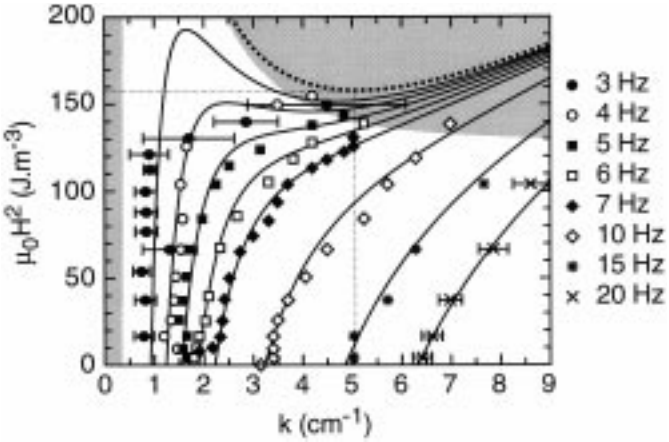

Fig. 8. Dispersion equation in the $(k, \mu_0 H^2)$ plane for different frequencies. The black lines represent the theoretical dispersion equation with $\sigma = 60$ mN/m; the thick dotted line is the theoretical marginal curve of stability (null frequency); the thin dotted lines locate the minimum of the marginal curve and read $k_c = 5.1$ cm^{-1} and $H_c = 11.2$ kA/m. The shaded area represents the frequency domain where viscosity effects become non negligible ($Re < 10$). For clarity purpose, only a few error bars have been plotted.

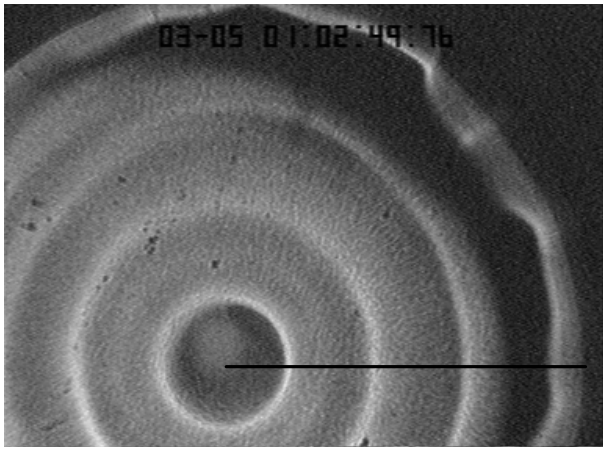

Fig. 9. Spontaneous static deformation below the critical field ($H/H_c = 0.79$). The dark line represents the cut along which the spatio-temporal diagrams have been extracted (Figs. 10 and 11).

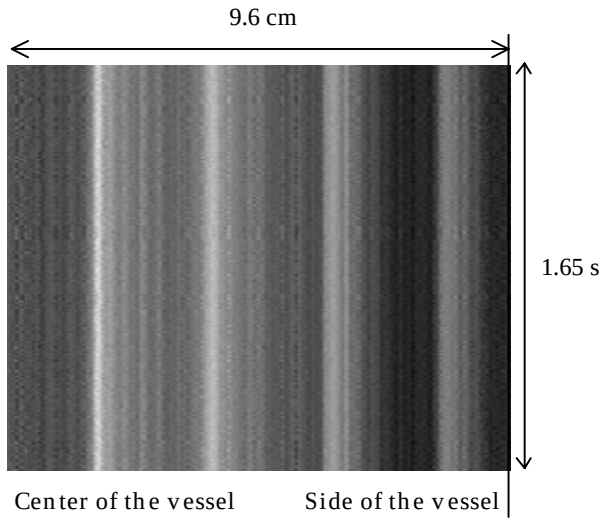

Fig. 10. Spatio temporal diagram of the spontaneous static deformation below the critical field ($H/H_c = 0.79$).

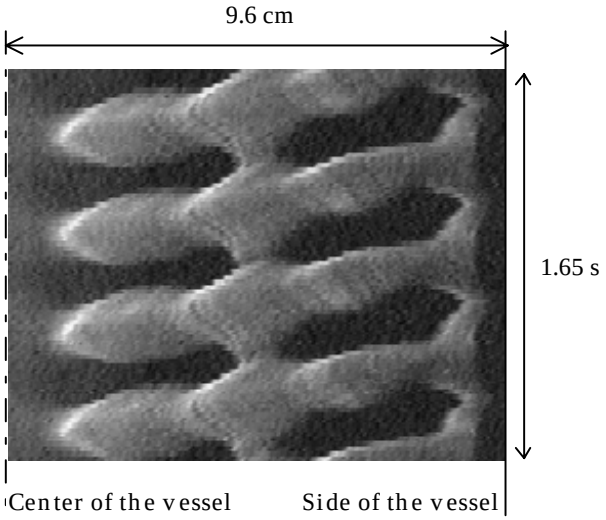

Fig. 11. Spatio temporal diagram of a 2.5 Hz wave propagating onto the spontaneous static deformation below the critical field at $H = 0.79 H_c$. The measurement of the wavelength is full of uncertainty.

on the distance from the radius). Although the surface is deformed, waves emitted from the edges of the ferrofluid container propagate onto this deformation (Fig. 11). Unfortunately it renders the measurement of the wavelength more uncertain, especially when the wavelength of propagating waves is close to the characteristic length of the pattern – about 2.2 cm which correspond to a characteristic wavevector of 2.8 cm^{-1}. This value is close enough to k^* ($k^* \approx 0.58\, k_c \approx 2.9$ cm^{-1}) so that it may lead to think that this phenomenon is correlated to the non-monotonicity of the dispersion curve in a way that is yet to be determined.

When the magnetic field is increased further close to the threshold ($H/H_c > 85\%$), the azimuthal symmetry of the system is broken and small azimuthal ripples form inside each wavecrest emitted from the edges (Fig. 12). The characteristic length of theses ripples is roughly the same as the wavelength of the emitted "parent" circular waves. Although their propagative behavior is erratic, we have found that the azimuthal ripples have the same frequency as the "parent" circular wave. Therefore a Faraday-like instability is unlikely to explain this phenomenon, as its frequency would be half of the driving frequency. A nonlinear theory should explain the presence of such ripples (in the linear theory there is no coupling between plane waves). The amplitude of the ripples increases with the magnetic field. If the magnetic field is sufficiently increased (to about 95% of the threshold value), the amplitude of the wavelets becomes so large that it masks the underlying parent circular wave. It is then unlikely to precisely

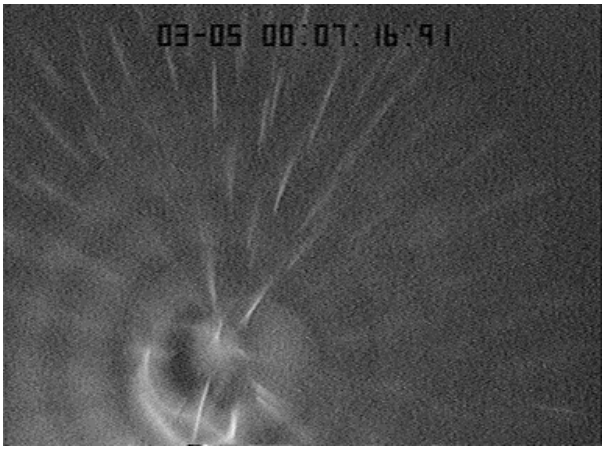

Fig. 12. Azimuthal ripples developing inside each wave crest emitted from the edges; their characteristic wavelength is of same order than the wavelength of the main radial wave.

determine the wave vector of the radial wave. Moreover the static radial deformation at these fields is very intense and the shadowgraph method fails to give a sharp image.

The sensitivity of the shadowgraph method has a drawback: when the peaks appear on the surface, it is so deformed that no image is given anymore. Because of the pre-transitional effects mentioned above (static deformation and azimuthal ripples), it is difficult to precisely assess the value of the threshold magnetic field H_c. Besides, an experiment with a direct visualization of the surface shows that the peaks don't appear simultaneously on the surface: when the field is increased to the threshold value, the peaks grow inward from the edges to the center of the cell (they start appearing on the edges at lower fields, because of the field gradient created by the presence of an edge). A precise estimation of the threshold magnetic field is dependent on the choice of a threshold criteria. We choose to keep the value of the magnetic field above which no image is visible anymore. This method provides a measurement of the threshold field of 11.5 kA/m which is merely 3% above of the expected value obtained from the fits in Figures 7 and 8.

5 Conclusion

We have designed a shadowgraph experiment in order to measure the dispersion equation of waves at the free surface of a magnetic fluid submitted to a vertical magnetic field. The model includes the specific magnetic behavior of the ferrofluid that we use, sensible boundary conditions and the effects of limited thickness. The agreement between theory and experience is satisfactory except in the region where the dispersion equation is non-monotonic. As a matter of fact, it is difficult to experimentally approach the non monotonic part of the dispersion curve: the emitted radial waves of interest are overcome by a static pattern and secondary azimuthal waves for a magnetic field close enough to its threshold value. The cause of these two phenomena is respectively assumed to be finite size effects and non-linear effects. However, it has not been determined if it could somehow be related to the non-monotonicity of the dispersion equation. This question remains open and will be the subject of forthcoming experiments.

We thank J. Servais and P. Lepert for their technical assistance. We thank O. Cardoso for the help provided in the conception and the tuning of the experimental setup. O. Sandre has to be thanked for granting us access to an accurate tensiometer. Fruitful discussions were made with B. Abou and R. E. Rosensweig.

References

1. M.D. Cowley, R.E. Rosensweig, J. Fluid Mech. **30**, 671 (1967).
2. B. Abou, J.-E. Weisfreid, S. Roux, J. Fluid Mech. (submitted).
3. A. Gailitis, J. Fluid. Mech. **82**, 401 (1977).
4. A.G. Boudouvis, J.L. Puchalla, L.E. Scriven, R.E. Rosensweig, J. Magn. Magn. Mater. **65**, 307 (1987).
5. J.-C. Bacri, D. Salin, J. Phys. Lett. France **45**, L559 (1984).
6. L.D. Landau, E.M. Lifshitz, *Statistical Physics*, Part 2, 3rd edn. (Pergamon Press, New York, 1980).
7. R.E. Rosensweig, J. Popplewell, *Electromagnetic forces and applications*, edited by J. Tani, T. Takagi (Elsevier, 1992), pp. 83–86.
8. R.E. Zelazo, J.R. Melcher, J. Fluid Mech. **39**, 1 (1969).
9. T. Mahr, A. Groisman, I. Rehberg, J. Magn. Magn. Mater. **159**, 45 (1996).
10. R.E. Rosensweig, *Ferrohydrodynamics* (Cambridge University Press, 1985).
11. This hypothesis is emitted by all authors, since it is impossible to analytically derive the demagnetizing factor otherwise.
12. B. Abou, G. Néron de Surgy, J.E. Weisfreid, J. Phys. II France **7**, 1159 (1997).
13. $H^{\rm i} = H^{\rm e} - DM$ where D is the demagnetization factor. In this geometry, $D = 1$.
14. $M = \chi H^{\rm i}$ and $H^{\rm e} = H^{\rm i} + M$ so $M = \chi/(1+\chi)H^{\rm e}$ whereas in [12] $M = \chi H^{\rm e}$.
15. F.H. Leblond, F. Mainardi, Acta Mech. **68**, 203 (1987).
16. R. Massart, IEEE Trans. Magn. **17**, 1247 (1981).
17. F.A. Tourinho, R. Franck, R. Massart, J. Mater. Sci. **25**, 3249 (1990).
18. S. Rasenat, G. Hartung, B.L. Winkler, I. Rehberg, Exp. Fluids **7**, 412 (1989).
19. Waves are damped but their frequency remains unaffected by viscosity at the first order.
20. The waves emitted at the edges of the vessel are likely to overcome any spontaneous Faraday ripple wave; see for example V.G. Bastovoi, R.E. Rosensweig, J. Magn. Magn. Mater. **122**, 234 (1993).
21. A.W. Adamson, *Physical Chemistry of Surfaces*, 4th edn. (Wiley & sons, 1982).